2024 European Control Conference (ECC)
June 25-28, 2024. Stockholm, Sweden

Frequency-domain properties of moving average and moving standard deviation with application to stage (motion) control

Marcel Heertjes[1]

Abstract— **In wafer scanners, moving average and moving standard deviation constitute time-domain measures that quantify scanning stage performance in terms of overlay and imaging. Though for control design a frequency-domain interpretation would be desirable to have, for moving standard deviation such an interpretation is not easily found. As a practical solution, an analytical expression for the response to single sinusoidal input will be derived. For data from an industrial scanning stage the usefulness of such an expression and the insights obtained from it will be discussed.**

I. INTRODUCTION

In wafer scanners, *i.e.,* the lithography tools for the manufacturing of microchips, moving average and moving standard deviation are key operations for control performance specification [1]. Moving average filtering of the stage tracking errors is done to specify how well a new layer is exposed on top of a previous layer of the wafer, the latter is known as machine overlay (positioning accuracy of the exposure) and on-product overlay (positioning accuracy of the exposed features). Specifying overlay is done as microchips are constructed layer by layer. Alignment with respect to a previous layer is essential for the integrated circuits to work, *i.e.,* overlay impacts yield. Typical overlay specifications are 2-2.5 nanometer for memory and logic.

Moving standard deviation is used to express imaging. It refers to how features from a reticle containing a blueprint of the microchip are translated to features on the wafer. This translation relies (among others) on the principles of light diffraction, the wavelength, the properties of the optics like numerical aperture, and the photosensitive properties of resist that require a certain threshold in accumulated exposure dose [2], [3]. Improved imaging associates with less blurring of features [4]. Specifications on moving standard deviation of stages are in the range of a few nanometers or less.

To better understand the moving average and moving standard deviation operations in terms of stage tracking errors, a frequency-domain perspective is adopted [5]. The frequency-domain properties of a moving average operation are largely known [6], [7] and resemble to some extent those of a first-order low-pass filter. In the absence of superposition the moving standard deviation operation viewed as a nonlinear input-output system does not admit a Laplace transform. As such a frequency-domain interpretation is lacking, though many practitioners tend to give the moving standard deviation operation high-pass filter properties [1]. The main contribution of this paper is an analytical expression of the moving standard deviation its response to sinusoidal input. Such an expression allows for a frequency-domain interpretation that offers insights in the response obtained from numerically computing the moving standard deviation operation for representative inputs. This will be show-cased on tracking error data taken from an industrial stage system.

The paper is further organized as follows. In Section II the moving average operation will be discussed. This is followed in Section III by a discussion on the moving standard deviation operation along with the derivation of its nonlinear frequency response. In Section IV the results will be demonstrated on measured time-series obtained from an industrial scanning stage system. In Section V the main conclusions will be summarized.

[1]Marcel Heertjes is with Department of Mechanical Engineering, Dynamics & Control group and Control Systems Technology group, Eindhoven University of Technology, 5600 MB Eindhoven, The Netherlands m.f.heertjes@tue.nl

II. MOVING AVERAGE

In wafer scanners moving average is used as a measure for machine overlay [2, Section 5.7], *i.e.,* the accuracy by which one layer of a wafer (upon reentering the wafer scanner) can be exposed on top of the previous layer.

Definition 2.1: In continuous time, the moving average operation $\mathscr{M}_A\{e(t)\}$ maps the tracking error signal e to the moving average signal e_{MA} via the linear (but non-causal) mapping

$$e_{MA}(t) \triangleq \frac{1}{\tau_{slit}} \int_{t-\tau_{slit}/2}^{t+\tau_{slit}/2} e(\tau) d\tau, \tag{1}$$

with time constant $\tau_{slit} > 0$; see also [8].

For wafer scanners, τ_{slit} represents the exposure time, which is defined as the ratio between slit length $d_{slit} > 0$ of the light source and scanning velocity $v_{max} > 0$, *i.e.,* $\tau_{slit} = d_{slit}/v_{max}$. To study the properties of the moving average operation in frequency domain, consider the next result.

Theorem 2.1: Let $\mathscr{F}\{e(t)\}$ and $\mathscr{F}\{e_{MA}(t)\}$, respectively, denote the Fourier transforms of the tracking error signal e and the moving average signal e_{MA} from (1). The moving average frequency response function $\mathscr{M}_A$ then reads

$$\mathscr{M}_A(\omega) \triangleq \frac{\mathscr{F}\{e_{MA}(t)\}}{\mathscr{F}\{e(t)\}} = \frac{2}{\omega\tau_{slit}} \cdot \sin\Big(\frac{\omega\tau_{slit}}{2}\Big), \tag{2}$$

which equals the (normalized) cardinal sine function $\sin(\pi x)/\pi x$ with $x = f\tau_{slit}$, and $f = \omega/2\pi$.

Copyright ©2024 EUCA

Proof: The proof follows from

$$\begin{aligned}\mathscr{F}\{e_{MA}(t)\} &= \int_{-\infty}^{\infty} \underbrace{\left\{\frac{1}{\tau_{slit}}\int_{t-\tau_{slit}/2}^{t+\tau_{slit}/2} e(\tau)d\tau\right\}}_{a*b} \underbrace{e^{-j\omega t}}_{c} dt \\ &= \int_{-\infty}^{\infty} \underbrace{e(t)}_{a} \underbrace{\left\{\frac{1}{\tau_{slit}}\int_{t-\tau_{slit}/2}^{t+\tau_{slit}/2} e^{-j\omega\tau}d\tau\right\}}_{b*c} dt,\end{aligned} \tag{3}$$

which gives

$$\begin{aligned}&\mathscr{F}\{e_{MA}(t)\} = \int_{-\infty}^{\infty} e(t)\left\{\frac{1}{\tau_{slit}}\int_{t-\tau_{slit}/2}^{t+\tau_{slit}/2} e^{-j\omega\tau}d\tau\right\}dt \\ &= \int_{-\infty}^{\infty} \frac{e(t)}{\tau_{slit}}\left\{-\frac{1}{j\omega}e^{-j\omega\tau}\Big|_{t-\tau_{slit}/2}^{t+\tau_{slit}/2}\right\}dt \\ &= \frac{2}{\omega\tau_{slit}}\int_{-\infty}^{\infty} e(t)\left\{e^{-j\omega t}\left(\frac{1}{2j}e^{j\omega\tau_{slit}/2} - \frac{1}{2j}e^{-j\omega\tau_{slit}/2}\right)\right\}dt \\ &= \frac{2}{\omega\tau_{slit}}\cdot\sin\left(\frac{\omega\tau_{slit}}{2}\right)\cdot \underbrace{\int_{-\infty}^{\infty} e(t)\cdot e^{-j\omega t}dt}_{\mathscr{F}\{e(t)\}},\end{aligned} \tag{4}$$

and which completes the proof. ■

Some useful properties of $\mathscr{M}_A$ in (2) are:

1) $\mathscr{M}_A(\omega)\to 1$, for $\omega\to 0$,
2) $|\omega\cdot\mathscr{M}_A(\omega)|\le\eta$ with uniform bound $\eta>0$, because $\mathscr{M}_A(\omega)\propto 1/\omega$, for $\omega\to\infty$,
3) $\mathscr{M}_A(\omega)$ is real-valued, giving zero phase shift for $\omega\tau_{slit}/2\in[2i\pi,\pi+2i\pi)$ with $i\in\mathbb{N}$, and minus 180 degrees phase shift for $\omega\tau_{slit}/2\in[\pi+2i\pi,2(i+1)\pi)$,
4) no spectral content at $\omega_i=2\pi i/\tau_{slit}$, $i\in\mathbb{N}\backslash\{0\}$.

To illustrate these properties, consider the Bode diagram in Fig. 1 of the moving average filter operation in (1). The figure

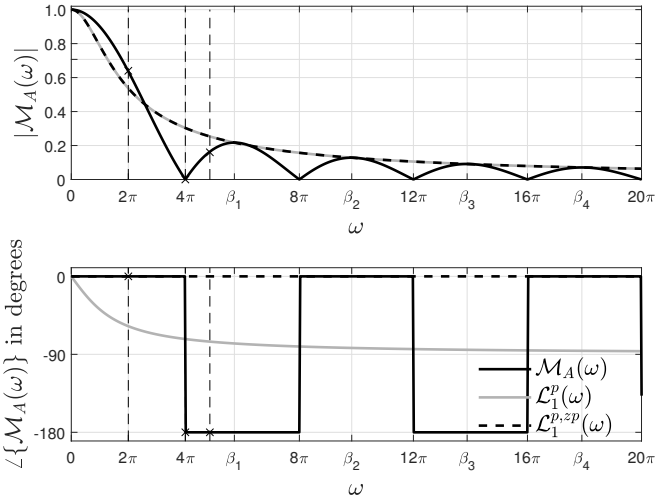

Fig. 1: Bode diagram of $\mathscr{M}_A(\omega)$ in (2) with $\tau_{slit}=0.5$.

also shows the frequency response function of a first-order low-pass filter $\mathscr{L}_1^p(\omega)\in\mathbb{C}^n$ (grey curve) and its real-valued counterpart $\mathscr{L}_1^{p,zp}(\omega)\in\mathbb{R}^n$ with zero phase (dashed curve):

$$\begin{aligned}\mathscr{L}_1^p(\omega) &= \frac{1}{j\omega\tau_{slit}/2+1} \\ \mathscr{L}_1^{p,zp}(\omega) &= \left|\mathscr{L}_1^p(\omega)\right| = \frac{1}{\sqrt{\omega^2\tau_{slit}^2/4+1}}.\end{aligned} \tag{5}$$

Note that for $\omega\to\infty$, $|\mathscr{M}_A(\omega)|\le|\mathscr{L}_1^p(\omega)|=|\mathscr{L}_1^{p,zp}(\omega)|$, which indicates first-order low-pass properties of $|\mathscr{M}_A(\omega)|$.

Remark 2.1: For harmonic input $e(t)=\hat{e}\sin(\omega t)$, time-domain integration of (1) gives

$$\begin{aligned}e_{MA}(t) &= \frac{1}{\tau_{slit}}\int_{t-\frac{\tau_{slit}}{2}}^{t+\frac{\tau_{slit}}{2}}\hat{e}\sin(\omega\tau)d\tau \\ &= -\frac{1}{\omega\tau_{slit}}\cdot\hat{e}\cos(\omega\tau)\Big|_{t-\frac{\tau_{slit}}{2}}^{t+\frac{\tau_{slit}}{2}} \\ &= -\frac{1}{\omega\tau_{slit}}\cdot\left(\underbrace{\hat{e}\cos\left(\omega t+\frac{\omega\tau_{slit}}{2}\right)}_{c(\alpha+\beta)=c(\alpha)c(\beta)-s(\alpha)s(\beta)} \overbrace{-\hat{e}\cos\left(\omega t-\frac{\omega\tau_{slit}}{2}\right)}^{c(\alpha-\beta)=c(\alpha)c(\beta)+s(\alpha)s(\beta)}\right) \\ &= \underbrace{\frac{2}{\omega\tau_{slit}}\cdot\sin\left(\frac{\omega\tau_{slit}}{2}\right)}_{=\mathscr{M}_A(\omega)}\cdot\hat{e}\sin(\omega t),\end{aligned} \tag{6}$$

which matches with the frequency response function $\mathscr{M}_A$ of Theorem 2.1.

From tracking control perspective, it is important to note that the physical interpretation of tracking error through the moving average filter operation is compromised by (a) low-pass (amplitude) filtering, (b) zero amplitude at integer multiples of $\omega=2\pi/\tau_{slit}$, and (c) its alternating change of sign (phase). Since $\mathscr{M}_A(\omega)\to 1$, for $\omega\to 0$, alignment, or DC tracking, is captured by moving average, hence its relation with overlay.

The moving average operation $\mathscr{M}_A$ in (2) naturally translates to autospectral density functions.

Definition 2.2: Let $\mathscr{G}_{ee}$ denote the one-sided autospectral density function of the error signal e, and $\mathscr{G}_{ee}^{MA}$ denote the corresponding autospectral density function of signal e_{MA}. Then both are defined as

$$\begin{aligned}\mathscr{G}_{ee}(\omega) &\triangleq \frac{2}{T}E\left\{|\mathscr{F}\{e(t)\}|^2\right\}, \text{ and} \\ \mathscr{G}_{ee}^{MA}(\omega) &\triangleq \frac{2}{T}E\left\{|\mathscr{F}\{e_{MA}(t)\}|^2\right\},\end{aligned} \tag{7}$$

with $E\{\cdot\}$ the expected value of the argument, and $T>0$ the record length.

For finite record length T, consider the mappings of the tracking error signal e, with $e=e_{MA}=0$ outside $t\in[0,T]$, onto the root-mean-square values e^{rms} and e_{MA}^{rms}, or

$$\begin{aligned}e_{(MA)}^{rms} &= \sqrt{\frac{1}{T}\int_0^T e_{(MA)}^2(t)dt} = \sqrt{\frac{1}{T}\int_{-\infty}^{\infty} e_{(MA)}^2(t)dt} \\ &= \sqrt{\frac{2}{T}\int_0^{\infty}|\mathscr{F}\{e_{(MA)}(t)\}|^2 d\omega} \triangleq \sqrt{\int_0^{\infty} G_{ee}^{(MA)}(\omega)d\omega},\end{aligned} \tag{8}$$

with the relation between G_{ee} and G_{ee}^{MA} given by

$$\begin{aligned}\mathscr{G}_{ee}^{MA}(\omega) &= \frac{2}{T}E\left\{\left|\frac{2\sin(\omega\tau_{slit}/2)}{\omega\tau_{slit}}\mathscr{F}\{e(t)\}\right|^2\right\} \\ &= \frac{2}{T}\cdot\frac{4\sin^2(\omega\tau_{slit}/2)}{\omega^2\tau_{slit}^2}\cdot E\left\{|\mathscr{F}\{e(t)\}|^2\right\} \\ &= \underbrace{\frac{4\sin^2(\omega\tau_{slit}/2)}{\omega^2\tau_{slit}^2}}_{=1-\gamma(\omega)}\mathscr{G}_{ee}(\omega).\end{aligned} \tag{9}$$

Observation 2.1: From (9) it is clear that e_{MA}^{rms} has no contribution from frequencies $f = i/\tau_{slit}$ with $i \in \mathbb{N}\backslash\{0\}$ where $1-\gamma(\omega)=0$, though $\mathscr{G}_{ee}(\omega = 2\pi f)$ may display a significant rate-of-change in power at these frequencies.
The frequency-dependent gain $0 \le \gamma(\omega) \le 1$, where $\gamma(0) = 0$, represents zero-phase high-pass filtering, which is shown in Fig. 2 with $\tau_{slit} = 0.5$. Alternatively, $1-\gamma(\omega)$ represents

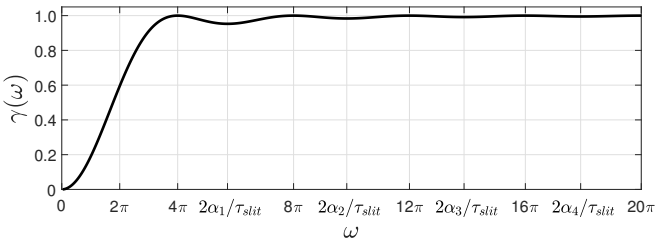

Fig. 2: High-pass properties of $\gamma(\omega)$ with $\tau_{slit} = 0.5$.

zero-phase low-pass filtering; see Appendix A for the local minima of $\gamma(\omega)$ derived at $2\alpha_i/\tau_{slit}$ with $i \in \{1,2,3,4,\dots\}$.

III. Moving standard deviation

In wafer scanners the moving standard deviation filter operation is used as a measure for imaging [1], *i.e.,* the degree of blurriness of the exposed features on a wafer, which is for example expressed by line-edge roughness.

Definition 3.1: In continuous time, the moving standard deviation operation $\mathscr{M}_{SD}\{e(t)\}$ maps the tracking error signal e to the moving standard deviation signal e_{MSD}, or $e \mapsto e_{MSD}$, via the root-mean-square (non-causal) mapping

$$e_{MSD}(t) \triangleq \sqrt{\frac{1}{\tau_{slit}}\int_{t-\frac{\tau_{slit}}{2}}^{t+\frac{\tau_{slit}}{2}}(e(\tau)-e_{MA}(t))^2 d\tau} \ge 0. \tag{10}$$

Lemma 3.1: Given Definitions 2.1 and 3.1, (10) equals

$$e_{MSD}(t) = \sqrt{\frac{1}{\tau_{slit}}\int_{t-\frac{\tau_{slit}}{2}}^{t+\frac{\tau_{slit}}{2}} e^2(\tau)d\tau - e_{MA}^2(t)}. \tag{11}$$

Proof: Given (1) and (10), it follows that

$$\begin{aligned}e_{MSD}^2(t) &= \frac{1}{\tau_{slit}}\int_{t-\frac{\tau_{slit}}{2}}^{t+\frac{\tau_{slit}}{2}} e^2(\tau)d\tau \\ &\quad - 2e_{MA}(t)\frac{1}{\tau_{slit}}\int_{t-\frac{\tau_{slit}}{2}}^{t+\frac{\tau_{slit}}{2}} e(\tau)d\tau + e_{MA}^2(t) \\ &= \frac{1}{\tau_{slit}}\int_{t-\frac{\tau_{slit}}{2}}^{t+\frac{\tau_{slit}}{2}} e^2(\tau)d\tau - e_{MA}^2(t).\end{aligned} \tag{12}$$

Taking the square root completes the proof. ∎

From Lemma 3.1 (and apart from the overall square root) the moving standard deviation error signal e_{MSD} can be interpreted as the difference between the moving average of the squared tracking error and the squared value of the moving average of the tracking error itself. As a result, if e_{MA} is small within some time interval $t \in [t_1, t_2]$, e_{MSD} tends to the root-mean-square value of the error signal e in that same time interval.

The root-mean-square value e_{MSD}^{rms} of the moving standard deviation error signal e_{MSD} follows from the next result.

Proposition 3.1: For $e_{MSD}(t) = 0$ outside $t \in [0,T]$ and for finite but sufficiently large record length $T/\tau_{slit} \gg 1$,

$$\begin{aligned}e_{MSD}^{rms} &\triangleq \sqrt{\frac{1}{T}\int_0^T e_{MSD}^2(t)dt} \\ &\approx \int_0^\infty \overbrace{\left\{1 - \frac{4\sin^2(\omega\tau_{slit}/2)}{\omega^2\tau_{slit}^2}\right\}}^{\gamma(\omega)}\mathscr{G}_{ee}(\omega)d\omega.\end{aligned} \tag{13}$$

Proof: For $e_{MSD} \mapsto e_{MSD}^{rms}$, it follows that

$$\begin{aligned}e_{MSD}^{rms} &\triangleq \sqrt{\frac{1}{T}\int_0^T e_{MSD}^2(t)dt} = \sqrt{\frac{1}{T}\int_{-\infty}^{\infty} e_{MSD}^2(t)dt} \\ &= \sqrt{\frac{1}{T}\int_{-\infty}^{\infty}\left\{\frac{1}{\tau_{slit}}\int_{t-\frac{\tau_{slit}}{2}}^{t+\frac{\tau_{slit}}{2}} e^2(\tau)d\tau - e_{MA}^2(t)\right\}dt} \\ &\approx \sqrt{\frac{1}{T}\int_{-\infty}^{\infty}\left\{e^2(t) - e_{MA}^2(t)\right\}dt} \ \text{(with } T/\tau_{slit} \gg 1\text{)}.\end{aligned} \tag{14}$$

Using (9), (14) becomes

$$\begin{aligned}e_{MSD}^{rms} &\approx \sqrt{\int_0^\infty \{G_{ee}(\omega) - G_{ee}^{MA}(\omega)\}d\omega} \\ &= \sqrt{\int_0^\infty \gamma(\omega)\mathscr{G}_{ee}(\omega)d\omega}.\end{aligned} \tag{15}$$

∎

Observation 3.1: e_{MSD}^{rms} in (13) equals high-pass filtering of $\mathscr{G}_{ee}$ by $\gamma(\omega)$, recall Fig.2. For $\omega \to \infty$, e_{MSD}^{rms} solely depends on the rate-of-change in power of $\mathscr{G}_{ee}$ as $\gamma(\omega) \to 1$.

Observation 3.2: The value e_{MSD}^{rms} includes frequency contributions from frequencies $f_i = i/\tau_{slit}$, with $i \in \mathbb{N}\backslash\{0\}$, in contrast to e_{MA}^{rms} in (9), recall Observation 2.1. The autospectral density function $\mathscr{G}_{ee}$ at these frequencies is fully taken into account, *i.e.,* $\gamma(\omega_i = 2\pi f_i) = 1$, see Fig.2.

Though the value e_{MSD}^{rms} in (13) can be related to high-pass filtering of $\mathscr{G}_{ee}$ by $\gamma(\omega)$, the relation between $\mathscr{F}\{e_{MSD}(t)\}$ and $\mathscr{F}\{e(t)\}$ is not given by any linear transfer. However, for harmonic input $e(t) = \hat{e}\sin(\omega t)$, the interpretation of a frequency response of the moving standard deviation operation can be obtained by the following result, which constitutes the main contribution of this paper.

Theorem 3.1: Let $e(t) = \hat{e}\sin(\omega t)$, with $\hat{e} > 0$, then

$$\frac{e_{MSD}(t)}{\hat{e}} = \sqrt{\frac{1}{2} - \frac{\cos(2\omega t)\sin(\omega\tau_{slit})}{2\omega\tau_{slit}} + (\gamma(\omega)-1)\sin^2(\omega t)}. \tag{16}$$

Proof: From (11), it follows that

$$
\begin{aligned}
&e_{MA}^2(t)+e_{MSD}^2(t)\\
&=\frac{1}{\tau_{slit}}\int_{t-\frac{\tau_{slit}}{2}}^{t+\frac{\tau_{slit}}{2}}(\hat{e}\sin(\omega\tau))^2 d\tau\\
&=\frac{1}{\tau_{slit}}\left\{\frac{\hat{e}^2}{2}\tau-\frac{\hat{e}^2}{4\omega}\sin(2\omega\tau)\Big|_{t-\frac{\tau_{slit}}{2}}^{t+\frac{\tau_{slit}}{2}}\right.\\
&=\frac{\hat{e}^2}{\tau_{slit}}\left(\frac{\tau_{slit}}{2}\underbrace{-\frac{1}{4\omega}\sin(2\omega t+\omega\tau_{slit})}_{s(\alpha+\beta)=s(\alpha)c(\beta)+c(\alpha)s(\beta)}\overbrace{+\frac{1}{4\omega}\sin(2\omega t-\omega\tau_{slit})}^{s(\alpha-\beta)=s(\alpha)c(\beta)-c(\alpha)s(\beta)}\right)\\
&=\frac{\hat{e}^2}{2}-\frac{\hat{e}^2\cos(2\omega t)\sin(\omega\tau_{slit})}{2\omega\tau_{slit}}.
\end{aligned}
\tag{17}
$$

Using $e_{MA}^2(t)=(1-\gamma(\omega))\hat{e}^2\sin^2(\omega t)$ completes the proof. ■

Theorem 3.1 shows that the response of the moving standard deviation operation to a sinusoidal input, *i.e.,* the power inferred by $e(t)=\hat{e}\sin(\omega t)$, is partially transferred to a DC component and partially to a component at double the input frequency ω as well as multiples thereof. None of its power is transferred to a component at the input frequency ω itself, which is in contrast to any linear frequency response. Other properties of (16) are:

1) $e_{MSD}\propto\hat{e}$, *i.e.,* homogeneity of degree 1,
2) $e_{MSD}=0$ for $\omega=0$, and
3) $e_{MSD}\to e_{MSD}^{rms}=\hat{e}/\sqrt{2}$ for $\omega\to\infty$.

Corollary 3.1: For harmonic error signals $e(t)=\hat{e}\sin(\omega t)$ with $\hat{e}>0$ and $\omega\geq 0$, $e_{MSD}(t)$ in (16) is strictly bounded by

$$
\underline{\eta}(\omega)\hat{e}\leq e_{MSD}(t)\leq\bar{\eta}(\omega)\hat{e},
\tag{18}
$$

with

$$
\begin{aligned}
\underline{\eta}(\omega)&=\min\left\{\sqrt{\frac{1}{2}-\frac{\sin(\omega\tau_{slit})}{2\omega\tau_{slit}}},\sqrt{\gamma(\omega)-\frac{1}{2}+\frac{\sin(\omega\tau_{slit})}{2\omega\tau_{slit}}}\right\},\\
\bar{\eta}(\omega)&=\max\left\{\sqrt{\frac{1}{2}-\frac{\sin(\omega\tau_{slit})}{2\omega\tau_{slit}}},\sqrt{\gamma(\omega)-\frac{1}{2}+\frac{\sin(\omega\tau_{slit})}{2\omega\tau_{slit}}}\right\}.
\end{aligned}
\tag{19}
$$

Proof: For arbitrary $\omega\in\mathbb{R}_{\geq 0}$, the extremes in the argument of (16) are found as roots of

$$
\begin{aligned}
&\frac{d}{dt}\left\{\frac{1}{2}-\frac{1}{2\omega\tau_{slit}}\cos(2\omega t)\sin(\omega\tau_{slit})+(\gamma(\omega)-1)\sin^2(\omega t)\right\}\\
&\quad=\sin(2\omega t)\left(-\frac{1}{\tau_{slit}}\sin(\omega\tau_{slit})+\omega(\gamma(\omega)-1)\right)=0.
\end{aligned}
\tag{20}
$$

Evaluating (16) at these roots, which are located at $2\omega t=i\pi$, with $i\in\mathbb{N}$, gives two type of solutions:

$$
\begin{aligned}
&\frac{1}{2}-\frac{\sin(\omega\tau_{slit})}{2\omega\tau_{slit}},\ \text{if } 2\omega t\in\{0,2\pi,4\pi,6\pi,\dots\},\ \text{or}\\
&\gamma(\omega)-\frac{1}{2}+\frac{\sin(\omega\tau_{slit})}{2\omega\tau_{slit}},\ \text{if } 2\omega t\in\{\pi,3\pi,5\pi,7\pi,\dots\}.
\end{aligned}
\tag{21}
$$

For any value $\omega\in\mathbb{R}_{\geq 0}$, (18) satisfies the bounds in (19). ■

$\bar{\eta}$ can be used to define the following frequency response magnitude for the moving standard deviation operation.

Definition 3.2: For $e(t)=\hat{e}\sin(\omega t)=e(t+T_p)$ and corresponding periodic $e_{MSD}(t)=e_{MSD}(t+T_p)$, with period time $T_p=1/f$, $f=\omega/2\pi$, the frequency response magnitude is defined as

$$
|\mathscr{M}_{SD}(\omega)|\triangleq\frac{\|e_{MSD}(t)\|_\infty}{\|e(t)\|_\infty}=\bar{\eta}(\omega).
\tag{22}
$$

Finally, the bounds in (18) can be transformed into

$$
\eta_{off}(\omega)\triangleq\frac{\underline{\eta}(\omega)+\bar{\eta}(\omega)}{2},\eta_{osc}(\omega)\triangleq\frac{\bar{\eta}(\omega)-\underline{\eta}(\omega)}{2}
\tag{23}
$$

$$
\begin{aligned}
\text{with } \underline{\eta}(\omega)&=\eta_{off}(\omega)-\eta_{osc}(\omega),\ \text{and}\\
\bar{\eta}(\omega)&=\eta_{off}(\omega)+\eta_{osc}(\omega),
\end{aligned}
\tag{24}
$$

where $\eta_{off}(\omega)$ represents at each ω the positive (and static) off-set part of $e_{MSD}(t)=e_{MSD}(t+T_p)$, with period time $T_p=1/f$, $f=\omega/2\pi$, whereas $\eta_{osc}(\omega)$, represents the magnitude of the oscillatory part.

The presented frequency-dependent functions: $|\mathscr{M}_A(\omega)|$ from (2), $\gamma(\omega)$ from Fig. 2, $\bar{\eta}(\omega)$ and $\underline{\eta}(\omega)$ from (19), $|\mathscr{M}_{SD}(\omega)|$ from (22), as well as $\eta_{off}(\omega)$ and $\eta_{osc}(\omega)$ from (23) are depicted in Fig. 3 where $\tau_{slit}=0.5$. The seemingly

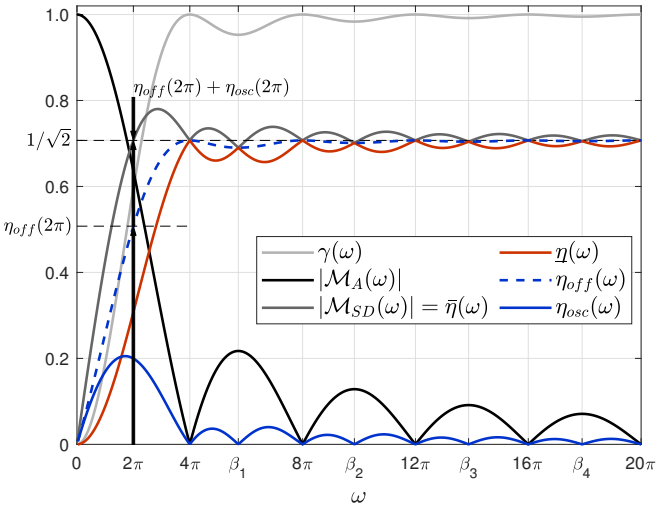

Fig. 3: Bode (magnitude) diagram for harmonic input only.

high-pass properties of $|\mathscr{M}_{SD}(\omega)|=\bar{\eta}(\omega)$ largely stem from the frequency-dependent off-set values in $\eta_{off}(\omega)$. Namely, the oscillatory part of $e_{MSD}(t)=e_{MSD}(t+T_p)$ captured by $\eta_{osc}(\omega)$ evidently shows low-pass behavior for $\omega\geq 2\pi$. Analytic expressions for the zeros of the oscillatory part are derived in Appendix B, *e.g.,* for β_i with $i\in\{1,2,3,4,\dots\}$.

Remark 3.1: In absence of superposition, $|\mathscr{M}_{SD}(\omega)|$ lacks the interpretation of a frequency response function and as such does not apply to inputs having multiple frequency components.

IV. Stage Control Example

To demonstrate the properties of the moving average and moving standard deviation filter operations consider

measured data collected from a short-stroke wafer stage of a wafer scanner; see [1] for a more detailed description of the working principle of wafer scanners and their components. The data are shown in Fig. 4 and represent

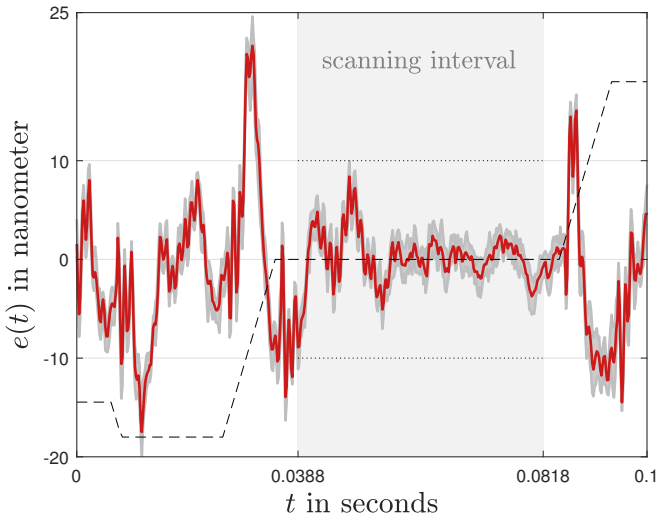

Fig. 4: Mean tracking error e and spread from 8 realizations.

the mean tracking error signal e (red curve) in the time interval $t \in [0, 0.1]$ seconds of 8 individually measured time-series along with the resulting spread (grey intervals). The sampling frequency is $f_s = 5$ kHz. The measured signals result from repeating an identical reference profile r of which its (scaled) acceleration characteristics are shown (dashed black). For non-zero acceleration the wafer stage is preparing for exposure. For zero acceleration levels, exposure takes place under constant (scanning) velocity, see the indicated interval $t \in [0.0388, 0.0818]$ seconds.

The data from Fig.4 after post-processing are shown in Fig. 5, which contains both the unfiltered (mean) error signal

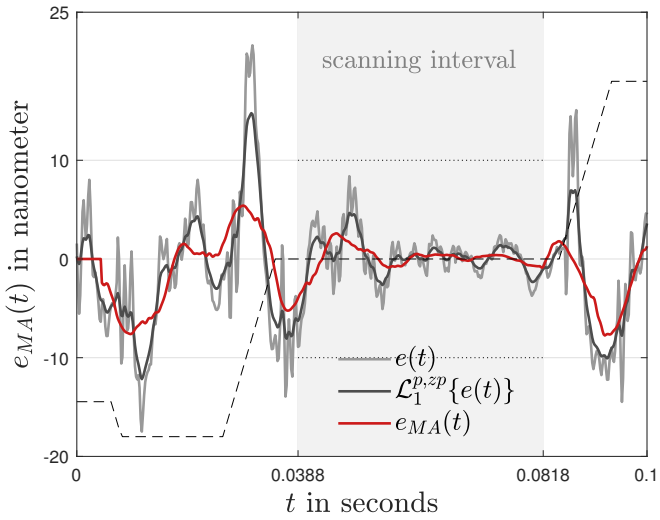

Fig. 5: Moving average; e_{MA} (red) from (1), mean tracking error e (grey), and $\mathcal{L}_1^{p,zp}\{e\}$ (black) from (5).

e (in gray) as well as the error signal e_{MA} (in red) obtained from a discrete-time moving average operation related to (1) with $\tau_{slit} = 9.2 \times 10^{-3}$ seconds. Notice that $5000 \times 9.2 \times 10^{-3}$ gives 46 samples in the moving average window. As such, the first zero of the moving average filter is found at $f = 5000/46 = 108.7$ Hz, which is a factor 20 below the sampling frequency, hence the validity of the continuous-time definition in (1). The figure also shows the error signal $\mathcal{L}_1^{p,zp}\{e\}$ (black) related to the first-order low-pass filter operation with zero phase as in (5). It can be concluded that e_{MA} partly shows first-order low-pass characteristics but these characteristics significantly differ from the first-order low-pass filter operation with zero phase in (5). In terms of magnitude, the moving average filter removes more low-frequency contents than justified by a first-order low-pass filter, and, in terms of phase, there appear multiple intervals where the moving average signal e_{MA} has opposite sign compared to the measured error signal e.

Fig. 6 contains both the unfiltered (mean) error signal $e(t)$ (gray) as well as the error signal $e_{MSD}(t)$ (red) obtained from applying a discrete-time version of the moving standard deviation operation in (10) with $\tau_{slit} = 9.2 \times 10^{-3}$s. It

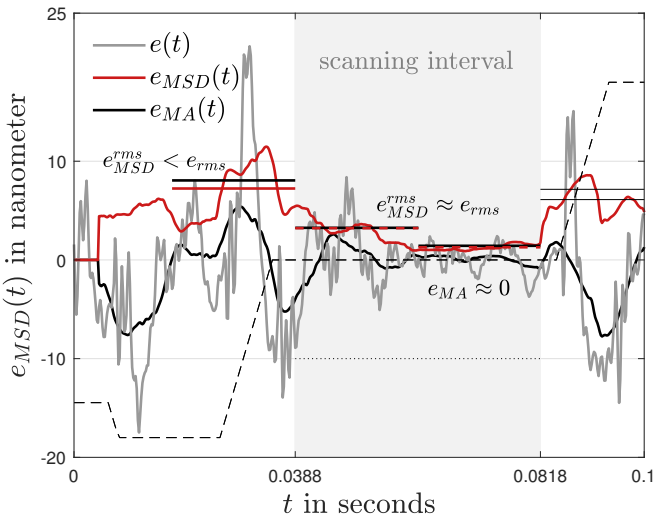

Fig. 6: Moving standard deviation; e_{MSD} (red curve) from (10), mean tracking error e (grey curve), e_{MA} (black curve) from (1), e_{MSD}^{rms} (red lines) from (13), and e^{rms} (black lines) from (8).

can be concluded that e_{MSD} shows low-pass characteristics regarding the high-frequency contents of $e(\omega)$, *i.e.,* the oscillatory part $\eta_{osc}(\omega)$ in (23), which is in line with the discussion regarding Definition III. Moreover, e_{MSD} tends to the root-mean-square value $e_{MSD}^{rms} \leq e_{rms}$ in subsequent time intervals; a record length of $T = 0.1$s is ten times larger than $\tau_{slit} = 9.2 \times 10^{-3}$s thereby validating the assumption underlying Proposition 13. This is especially clear toward the end of the scanning interval; recall the discussion on Lemma (3.1) and notice the moving average error $e_{MA}(t) \approx 0$ in the interval $t \in [0.05, 0.08]$ seconds. Prior to scanning, $e_{MA} \neq 0$ and $e_{MSD}^{rms} < e_{rms}$, *i.e.,* both low- and high-frequency content contribute to the power of the tracking error signal e.

In terms of power spectral density (PSD) analysis, Fig.

7 demonstrates that: (a) e_{MSD} is a measure of power that

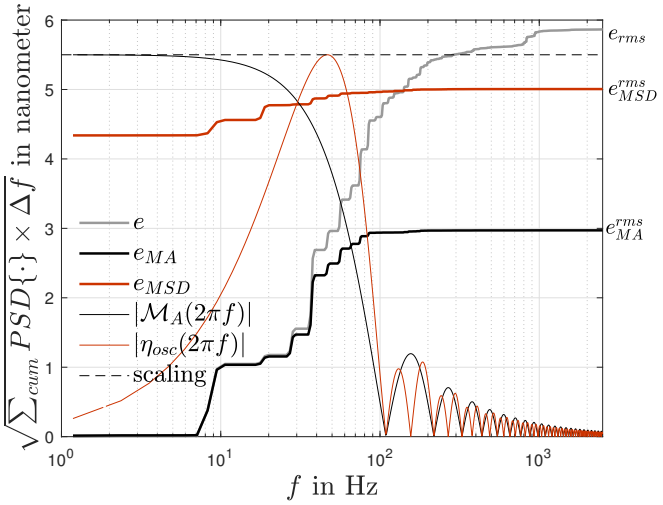

Fig. 7: Cumulative power spectral densities (PSD); e_{MSD} (red) from (10), e (grey), and e_{MA} (black) from (1) along with the (scaled) filters $\mathscr{M}_A$ (thin black) and η_{osc} (thin red).

through its DC contribution captures most of the root-mean-square value of $e^{rms}_{MSD} \leq e_{rms}$, (b) both e_{MSD} and e_{MA} show low-pass properties when compared to the unfiltered tracking error e, and (c) at the roots ω_i of $|\mathscr{M}_A(\omega_i)|, |\eta_{osc}(\omega_i)| = 0$, e_{MA} and e_{MSD} show no change of power while e does.

V. CONCLUSIONS

As main takeaway of the moving average and moving standard deviation analysis in frequency domain it was found that both operations have a frequency response that has properties that can be partly explained by first-order low-pass filtering. Different are the specific frequencies related to the moving time interval where the frequency response has no frequency content at all. Also, the phase shift of the frequency response alternates for different frequencies between zero and 180 degrees meaning that the moving average error signal can have opposite signs when compared to the unfiltered tracking error signal. The moving standard deviation operation provides a moving estimate of power of its mainly high-frequency content.

APPENDIX A

The frequency-dependent gain $\gamma(\omega)$ in Fig. 2 has local minima at frequencies ω_i where

$$\begin{aligned}&\left\{\frac{\partial\gamma(\omega)}{\partial\omega}\right\}_{\omega=\omega_i}\\ &= -\frac{4\sin(\omega_i\tau_{slit}/2)\cos(\omega_i\tau_{slit}/2)}{\omega_i^2\tau_{slit}} + \frac{8\sin^2(\omega_i\tau_{slit}/2)}{\omega_i^3\tau_{slit}} = 0\\ &\implies \tan\left(\frac{\omega_i\tau_{slit}}{2}\right) = \frac{\omega_i\tau_{slit}}{2}.\end{aligned} \tag{25}$$

As (25) has no solutions in closed form, one has to reside to numerical approximation, see Table I. These minima are shown in Fig. 2 for $\omega > 0$ and $\tau_{slit} = 0.5$ at $\omega_i = 4\alpha_i$, $i \in \mathbb{N}\backslash\{0\}$. Notice that $\lim_{i\to\infty}\alpha_i = (i+0.5)\pi$, $i \in \mathbb{N}\backslash\{0\}$.

TABLE I: Numerically approximated local minima of $\gamma(\omega)$ as solutions of $\tan(\alpha_i) = \alpha_i$ with $\omega_i = 2\alpha_i/\tau_{slit}$.

i	α_i	$\gamma(\omega_i)$
1	1.430π	0.811
2	2.459π	0.934
3	3.471π	0.967
4	4.477π	0.980
5	5.482π	0.987
.	.	.
n	$(n+0.5)\pi$	1

APPENDIX B

The oscillatory part of $e_{MSD}(t)$ represented by $\eta_{osc}(\omega)$ is zero at frequencies $\omega = \omega_i$, which are the roots of

$$\sqrt{\gamma(\omega) - \frac{1}{2} + \frac{\sin(\omega\tau_{slit})}{2\omega\tau_{slit}}} = \sqrt{\frac{1}{2} - \frac{\sin(\omega\tau_{slit})}{2\omega\tau_{slit}}}. \tag{26}$$

First, $\omega_i = 0$ gives $\mathscr{M}_{SD}(0) = 0$, which follows from $\lim_{\beta\to 0}\sin(\beta/2)/\beta = 1/2$ with $\beta = 2\omega\tau_{slit}$. Second, (26) has a solution at $\omega \to \infty$, for which holds that $\lim_{\omega\to\infty}\eta_{off}(\omega) = 1/\sqrt{2}$. Third, $\omega_i = 2\pi f_i$ with $f_i = i/\tau_{slit}$, $i \in \mathbb{N}\backslash\{0\}$, render $\mathscr{M}_{SD}(\omega_i) = 1/\sqrt{2}$ as $\gamma(\omega_i) = 1$ and $\sin(\omega_i\tau_{slit}) = 0$. Fourth, solutions are found at $\beta_i = 2\omega_i\tau_{slit} = 2\alpha_i/\tau_{slit}$, as (26) yields

$$\begin{aligned}&\gamma(\omega_i) - 1 + \frac{\sin(\beta_i/2)}{\beta_i} = -\frac{\sin(\beta_i/2)}{\beta_i}\\ &\qquad\implies \tan(\alpha_i) = \alpha_i,\ \ \alpha_i = \omega_i\tau_{slit}/2.\end{aligned} \tag{27}$$

The values of $\beta_i = 4\alpha_i$ (with α_i from Table I) and $\mathscr{M}_{SD}(\omega_i)$ are shown in Table II.

TABLE II: Numerically approximated local minima of $|\mathscr{M}_{SD}(\omega_i)|$ as solutions of $\tan(\alpha_i) = \alpha_i$.

i	$\beta_i = 4\alpha_i$	$\lvert\mathscr{M}_{SD}(\omega_i)\rvert$
1	$4\cdot 1.430\pi$	0.6901
2	$4\cdot 2.459\pi$	0.7013
3	$4\cdot 3.471\pi$	0.7042
4	$4\cdot 4.477\pi$	0.7053
5	$4\cdot 5.482\pi$	0.7059
⋮	↓	↓
n	$4\cdot(n+0.5)\pi$	$1/\sqrt{2}$

REFERENCES

[1] H. Butler, Position control in lithographic equipment, IEEE Control Systems Magazine, vol. 31, no. 5, pp. 28-47, 2011.

[2] H.J. Levinson, Principles of Lithography; third edition. SPIE press, Bellingham, WA, 2010.

[3] B.J. Lin, Optical Lithography - Here is Why, Second edition, SPIE Press, Bellingham, WA, 2021.

[4] H.J. Levinson, Lithography Process Control, Tutorial Texts in Optical Engineering, vol. TT28, SPIE Press, Bellingham, WA, 1999.

[5] A. Carbone and K. Kiyono, Detrending moving average algorithm: frequency response and scaling performances, Physical Review E, vol. 93, no. 6, pp.1-12, 2016.

[6] W. Sun, J-X Shen, K. Wang, and M-J Jin, Motor control application of fixed-sampling-interval and fixed-depth moving average filters, IEEE Trans. on Industry Applications, vol. 52, no. 2, pp. 1831-1841, 2016.

[7] S. Golestan, M. Ramezani, J.M. Guerrero, F.D. Freijedo, and M. Monfared, Moving average filter based phase-locked loops: performance analysis and design guidelines, IEEE Trans. on Power Electronics, vol. 29, no. 6, pp. 2750-2763, 2014.

[8] R. Hyndman, Moving Averages, International Encyclopedia of Statistical Science, pp.866-869, 2010.